MICROCOPY RESOLUTION TEST CHART
NATIONAL BUREAU OF STANDARDS-1963-A

AD A126204

CREATION OF HIGH ENERGY ELECTRON TAILS

DUE TO THE MODIFIED TWO-STREAM INSTABILITY.

by

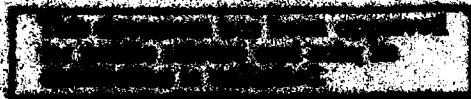Motohiko Tanaka and K. Papadopoulos

March 1983

UNIVERSITY OF MARYLAND
DEPARTMENT OF PHYSICS AND ASTRONOMY

REPORT DOCUMENTATION PAGE		READ INSTRUCTIONS BEFORE COMPLETING FORM
1. REPORT NUMBER University of Maryland Report AP83-048	2. GOVT ACCESSION NO. AD. A126 204	3. RECIPIENT'S CATALOG NUMBER
4. TITLE (and Subtitle) CREATION OF HIGH ENERGY ELECTRON TAILS DUE TO THE MODIFIED TWO-STREAM INSTABILITY		5. TYPE OF REPORT & PERIOD COVERED Interim report on a continuing problem
		6. PERFORMING ORG. REPORT NUMBER
7. AUTHOR(s) Motohiko Tanaka and K. Papadopoulos		8. CONTRACT OR GRANT NUMBER(s) N00014-79C-0665
9. PERFORMING ORGANIZATION NAME AND ADDRESS University of Maryland Department of Physics and Astronomy College Park, Maryland 20742		10. PROGRAM ELEMENT, PROJECT, TASK AREA & WORK UNIT NUMBERS
11. CONTROLLING OFFICE NAME AND ADDRESS Office of Naval Research NASA Arlington, VA 22217 Washington, D.C.		12. REPORT DATE March 1983
		13. NUMBER OF PAGES 14
14. MONITORING AGENCY NAME & ADDRESS(if different from Controlling Office)		15. SECURITY CLASS. (of this report) UNCLASSIFIED
		15a. DECLASSIFICATION/DOWNGRADING SCHEDULE

16. DISTRIBUTION STATEMENT (of this Report)

Approved for public release; distribution unlimited.

17. DISTRIBUTION STATEMENT (of the abstract entered in Block 20, if different from Report)

18. SUPPLEMENTARY NOTES

To be published in Physics of Fluids.

19. KEY WORDS (Continue on reverse side if necessary and identify by block number)

Modified two stream instabilities
Nonlinear plasma theory
Electron acceleration

20. ABSTRACT (Continue on reverse side if necessary and identify by block number)

Particle simulations of the modified two-stream instability demonstrate strong electron acceleration rather than bulk heating when the relative drift speed v_d is below a critical speed V_c. A very interesting nonlinear autoresonance acceleration process is observed which accelerates the electrons much above the phase speed of the linearly unstable modes. Simple criteria are presented that predict the value of V_c and the number density of the accelerated electrons.

DD FORM 1473 EDITION OF 1 NOV 65 IS OBSOLETE
1 JAN 73

S/N 0102-LF-014-6601

CREATION OF HIGH ENERGY ELECTRON TAILS

DUE TO THE MODIFIED TWO-STREAM INSTABILITY

by

Motohiko Tanaka[1], K. Papadopoulos[2]

1. Institute for Physical Science and Technology
2. Department of Physics and Astronomy
University of Maryland, College Park, Maryland 20742

ABSTRACT

Particle simulations of the modified two-stream instability demonstrate strong electron acceleration rather than bulk heating when the relative drift speed v_d is below a critical speed V_c. A very interesting nonlinear autoresonance acceleration process is observed which accelerates the electrons much above the phase speed of the linearly unstable modes. Simple criteria are presented that predict the value of V_c and the number density of the accelerated electrons.

The modified two-stream instability has been studied rather extensively [1-3] as an important process that transfers ion cross-field drift energy to parallel electron energy when the electron ion drift speed v_d is lower than the local Alfven speed v_A. It is usually assumed in the literature that the electron energy transfer results in bulk electron heating. However, in this letter we demonstrate that in the low drift regime (i.e. $v_d \lesssim 3 v_i$, where $v_i = (2T_i/m_i)^{1/2}$ is ion thermal speed), the modified two-stream instability results in electron acceleration instead of electron heating (i.e. formation of suprathermal electron tails). This result has very important implications to many physical situations such as shock electron acceleration [4,5], critical ionization phenomena[6] and the more recently observed anomalous glow of the space shuttle[7]. The emphasis in this letter is on the physics of the tail formation as revealed by particle simulations rather than the applications which will be discussed elsewhere.

The simulations were performed in one dimension in a fashion similar to that of McBride et al.[3] Namely, the magnetic field (B_0) was tilted by an angle θ from the simulation axis (x-axis) such that the maximum linear growth of the instability occurs in this direction. A Darwin electromagnetic code with periodic boundary conditions and a large system (128 or 256 cells) was used for the computations. Finite size particles (50 electrons and ions in each cell) were assigned three velocity components randomly using a quiet start method. The electrons were treated as magnetized and the ions as unmagnetized. The ions had an initial cross-field drift $\underline{v}_d$ relative to the electrons, ranging from 2 to 5 times v_i, while the electrons were initially at rest. The cell size Δ was chosen as $\Delta = \sqrt{2}\lambda_e$ ($\lambda_e = v_e/\sqrt{2}\omega_{pe}$ is the Debye length

where $v_e = (2T_e/m_e)^{1/2}$ is electron thermal speed) and the particle size a_x as $a_x/L = 0.008$ where $L = 128\Delta$ or 256Δ is the system size. Other initial parameters were: electron cyclotron frequency $\omega_{ce} =$ electron plasma frequency ω_{pe}; ratio of electron temperature to ion temperature $T_e/T_i = 2/3$; ion beta $\beta = 8\pi nT_i/B_o^2 = 0.01$; mass ratio $m_i/m_e = 400$; the angle $\theta = 88^\circ$ for the $v_d/v_i = 2$ and $\theta = 85^\circ$ for $v_d/v_i = 5$ case, as given by the most unstable mode.

The time development of Fourier amplitudes of the electric field $E_x(t)$ normalized by $(8\pi nT_i)^{1/2}$ is shown in Fig. 1. (Results of the $v_d/v_i = 2$ run are described unless otherwise specified.) For this run ($L = 256\Delta$), approximately 30 modes are actually unstable; however, only the most unstable modes $m = 11, 12, 13$ are plotted. Between $\omega_{LH}t = 5$ and 15, the waves grow exponentially and saturate at about $\omega_{LH}t \sim 25$. At $\omega_{LH}t \sim 20$, the most dominant modes are $m = 10 \sim 15$. As will be noted later, the wave characteristics change drastically between $\omega_{LH}t = 20$ and 30 due to the wave-particle interactions. At $\omega_{LH}t \sim 30$, after saturation, the dominant modes are $m = 6 \sim 16$ and $m = 21 \sim 26$, while after $\omega_{LH}t \sim 35$ the wave amplitudes decrease slowly. To show contributions of the electric fields other than $m = 11 \sim 13$ at later times, electric field energy $\epsilon_E = \langle E_x^2 \rangle/8\pi$ is also plotted in Fig. 1.

The linear theory of the modified two-stream instability is described in the electrostatic limit by the dispersion equation[3]

$$D_{ES} \equiv 1 + (2\omega_{pe}^2/k^2 v_e^2) \, [1 + \zeta_0 Z(\zeta_0) \, I_0(\lambda)e^{-\lambda}]$$

$$+ \, (2\omega_{pi}^2/k^2 v_i^2) \, [1 + \zeta_i Z(\zeta_i)] = 0, \tag{1}$$

where $\zeta_0 = \omega/k_{\parallel}v_e$, $\zeta_1 = (\omega - kv_d \sin\theta)/kv_1$, $k_{\parallel} = k\cos\theta$, $Z(\zeta)$ is the plasma dispersion function and $I_0(\lambda)$ is the zero-th order modified Bessel function with $\lambda = k^2 v_e^2 \sin^2\theta/2\omega_{ce}^2$. The measured frequency and growth rate in our simulations, scaled by the lower-hybrid frequency ω_{LH}, are $\omega_r \sim 0.3\,\omega_{LH}$, $\gamma \sim 0.1\,\omega_{LH}$ for the most unstable mode, and the corresponding wavenumber k satisfies $kv_1/\omega_{LH} = kv_e/\omega_{ce}(T_i/T_e)^{1/2} \sim 0.4$, all of which agree well with the linear theory.

The distribution function of electron velocities parallel to the magnetic field at the end of the run is shown in Fig. 2. Superimposed on them are the corresponding ion perpendicular velocity distributions $f(v_{1i})$, where $v_{1i} = v_x/\cos\theta$. A well-developed high energy electron tail is formed with the maximum parallel speed of $v_{\parallel max} \sim 7v_e$ while little change occurs in the main part of electrons, which retains its Maxwellian shape centered at $v_{\parallel} = 0$. On the other hand, the initial drifting Maxwellian distribution of ions centered at

$v_{1i} = 4v_e$ evolves into double-peaked distribution which suggests strong ion trapping.

The phase space distributions of the electrons and ions are shown in Fig. 3. Plotted here are the electron parallel velocities (left column) and ion perpendicular velocities (right column) versus their position along the x direction. Distributions in other directions do not show significant changes except for a slight electron ExB drift and are not displayed here. Changes in the distributions begin to occur at $\omega_{LH}t \sim 15$ which is the start of the nonlinear stage. Between $\omega_{LH}t = 20$ and 30, electrons are rapidly accelerated along the magnetic field while ions become trapped by the waves. The electron phase space at $\omega_{LH}t = 30$ (Fig. 3b) shows 13 or 14 tails, about the same number as the mode number

(12) of the linearly most unstable wave. After $\omega_{LH}t \sim 30$, the electrons in the tails are slowly and monotonically accelerated without a significant bouncing motion, and they finally become untrapped and detached from the main body of electrons to form a high energy electron beam parallel to the magnetic field (see, Fig. 3c-e). The fastest electrons have energies $mv_{\parallel}^2/2 \sim 50\ T_{eo}$ which is 100 times the initial electron energy. Since the population of the electron beam is approximately 8% of the total electrons and their average energy is 36 T_{eo} or six times as much as the initial ion drift energy, the electron beam carries 60% of the total electron energy parallel to the magnetic field at the end of the run. The saturation mechanism of the instability is ion trapping, as seen in Fig. 3. The saturation amplitude is calculated from $|E_k| \sim k\ \phi_k$, $2e\phi_k \sim (m_i/2)[(v_d-\omega/k)^2+v_i^2/2]$. The theoretical saturation amplitude due to ion trapping is thus $(E/\sqrt{8\pi nT_i})_{th} \sim 0.14$ and the amplitude measured in the simulation is $(E/\sqrt{8\pi nT_i})_{obs} \sim 0.11$ for the $v_d/v_i = 2$ run.

The evolution of the wave characteristics and the electron tail formation are strongly coupled. Shown in Fig. 4 is the change in the parallel wave phase speed $v_{ph} = \omega/k_{\parallel}$ for Fourier modes $m = 10 \sim 13$ and 24. [The phase speed was calculated from the measured frequency ω.] The two solid lines represent the maximum speed of the electrons parallel to the magnetic field (denoted el. max) and the speed of the fastest 1% electrons on the tail (denoted el. 1%). As the linear theory predicts, the phase speeds of the unstable modes are all less than 1.5 v_e within the slope of the electron distribution before the instability sets in. This means that the electrons can resonantly interact with the waves. During the nonlinear growth of the instability ($\omega_{LH}t = 20 \sim 30$),

the phase speed of the wave always stays at the tip of the rapidly

rising electron tails of Fig. 3. During the same interval the phase

speed increases (i.e., there is nonlinear frequency shift) closely

followed by an increase in the velocities of the electrons in the

tail. When the phase speed reaches the drift speed, $v_d/\cos\theta = 4v_e$

(projected on the parallel direction), it stops increasing and stays

close to the drift speed for $\omega_{LH}t = 30 \sim 50$. After $\omega_{LH}t \sim 40$, slowly

growing waves with the mode numbers around 8 and 24 dominate and

continue to slowly accelerate the electrons. By increasing the ratio

v_d/v_i to larger than 3, we observed a gradual transition from tail

formation to bulk heating. Our results were similar to Ref. 3, for the

case $v_d/v_i = 5$, in which bulk electron heating occurs.

The observed critical speed $V_c = 3v_i$ below which electron

acceleration occurs, is consistent with considerations concerning

whether electrons or ions are trapped first [3,8]. The ratio of the

electron (ϕ_e) to ion (ϕ_i) trapping potential is given by

$$\phi_i/\phi_e = (m_i/m_e)(k_i/k)^2 \ (v_d - v_{ph})^2/v_{ph}^2 \tag{2}$$

where v_{ph} is the phase speed of the most unstable wave. For $\phi_i/\phi_e > 1$

electron trapping occurs first and saturates the instability resulting

in bulk electron heating. In the opposite case ($\phi_i/\phi_e < 1$), saturation

occurs by ion trapping and only a fraction of the electrons gain

energy. From (1) and the inequality $\phi_i/\phi_e < 1$, we find the condition

for tail formation as

$$0.6 < \frac{v_d}{v_i} \leq 3 \tag{3}$$

The lower inequality comes from the linear threshold. Our runs for $v_d/v_i = 3.5$ and 5.0 were characterized by flat topped electron distributions and absence of tails, which are consistent with the inequality (3).

The observed fraction of electrons being accelerated is almost equal to the fraction of electrons, that initially had velocity larger than the phase speed $v_{ph\parallel} = \omega/k_\parallel$ corresponding to the most unstable mode. For example, for the case $v_d/v_i = 2$ the above argument gives 9%, while the observed value was 8%. It is interesting to note that in this case the electron trapping width was $\delta v_T \approx 1.5\, v_e$, comparable to the parallel wave phase velocity. The lack of trapped orbits in the electron phase space indicates that the autocorrelation time was shorter than the trapping time. The simulation results indicate that a nonlinear autoresonance process operates accelerating electrons to their final energy. While the trapped ion dynamics control the saturation of the linearly unstable modes, the tail electrons (Fig. 3) control the nonlinear frequency shift, which results in an increase in the parallel phase speed shown in Fig. 4. This result is supported by our frequency spectral analysis which shows no frequency shift for the $v_d/v_i = 5$ case, contrary to the $v_d \leq V_c$ case.

In summary we have demonstrated that for $v_d \leq V_c \approx 3v_i$, the modified two-stream instability results in electron acceleration rather than the conventionally assumed electron heating. In this case ion trapping controls the instability saturation, while a small fraction of electrons are accelerated in the direction parallel to the magnetic field by a systematic nonlinear increase in the phase velocity. The simulations shown here were 1-D. Preliminary 2-D simulations, which

allow for a symmetric growth of the fields to the magnetic field show

development of similar electron tails. In this case, however, the tails

are on both sides of the electron distribution. These results along

with a detailed analysis of the autoacceleration process is under study

and will be discussed elsewhere.

Acknowledgement

References

1. A. B. Mikhailovskii and V. S. Tsypin, Zh. ETF Pis. Red., _3_, 247 (1966) [JETP Letters _3_, 158 (1966)].

2. N. A. Krall and P. C. Liewer, Phys. Fluids, _15_, 1166 (1972).

3. J. B. McBride, E. Ott, J. P. Boris and J. H. Orens, Phys. Fluids, _15_, 2367 (1975).

4. M. Lampe and K. Papadopoulos, Astrophys. J., _212_, 886 (1977).

5. K. Papadopoulos, Proc. of the International School on Plasma Astrophysics, Varenna (ESA SP-161) p. 313 (1981).

6. A. Galeev, ibid., p. 77 (1981); V. Formisano, A. Galeev, R. Sagdeev, Planet. Space Sci. _30_, 491 (1982).

7. K. Papadopoulos, Phys. Rev. Lett. (communicated).

8. M. Lampe, W. Manheimer and K. Papadopoulos, NRL memo report 3076 (1975).

Figure Captions

Fig. 1 Development of three most unstable Fourier amplitudes (labelled
by mode number) of the electric field normalized by
$(8 \pi n T_i)^{1/2}$ where n and T_i are initial density and ion
temperature. Also plotted is electric field energy
$\varepsilon_E = \langle E_x^2 \rangle / 8 \pi$.

Fig. 2 Electron parallel (solid) and ion perpendicular (dashed)
velocity distribution at $\omega_{LH} t = 60$. The ordinate is in a
linear scale.

Fig. 3 Phase space distributions of electrons $(v_\parallel/v_e$ vs x) (left) and
ions $(v_\perp/v_i$ vs x) (right) at $\omega_{LH} t = 20$, 30, 40, 50 and 60 from
top to bottom.

Fig. 4 Evolution of the wave phase speed parallel to the magnetic
field for modes m = 10 ~ 13 and 24. Top two lines represent
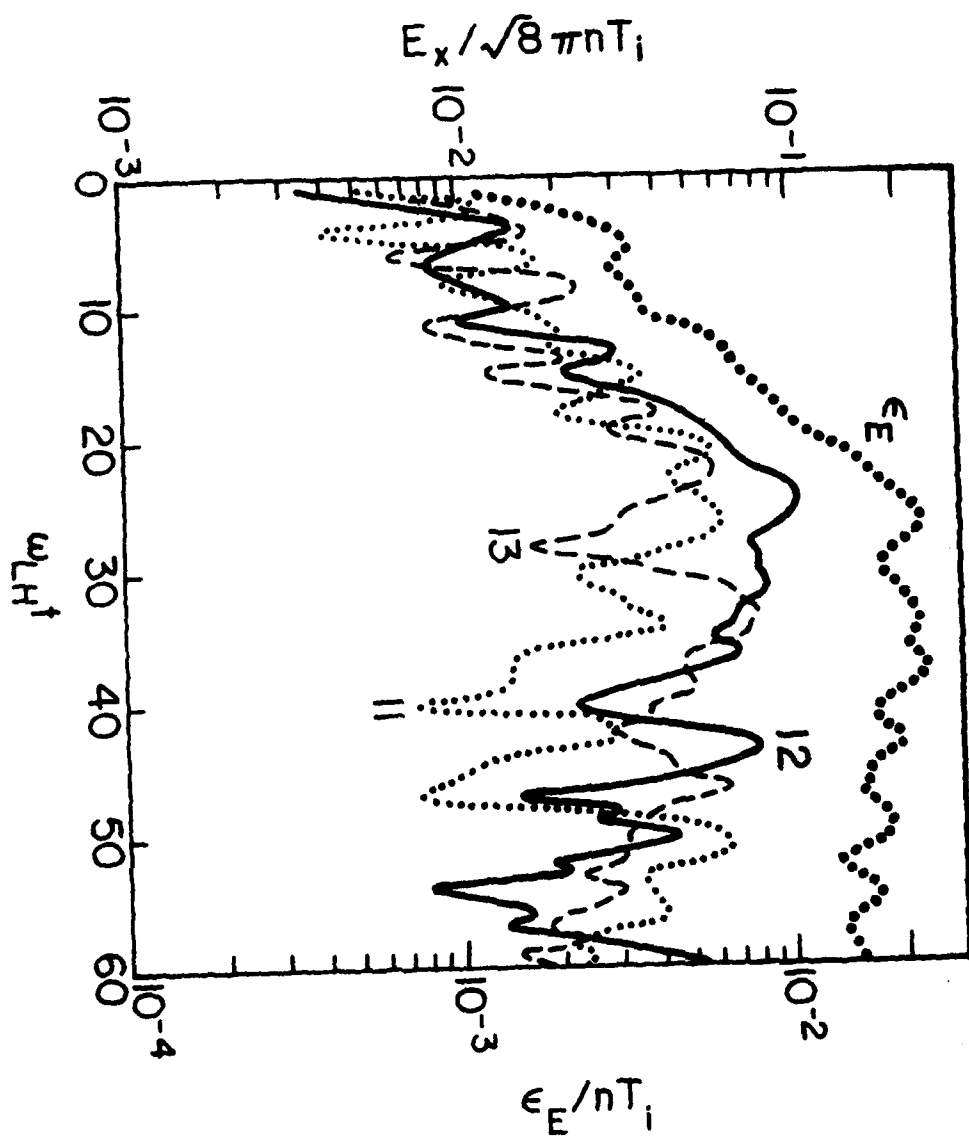the maximum electron speed and the speed of the fastest (1%)
electrons respectively.

Fig. 1

Fig. 2
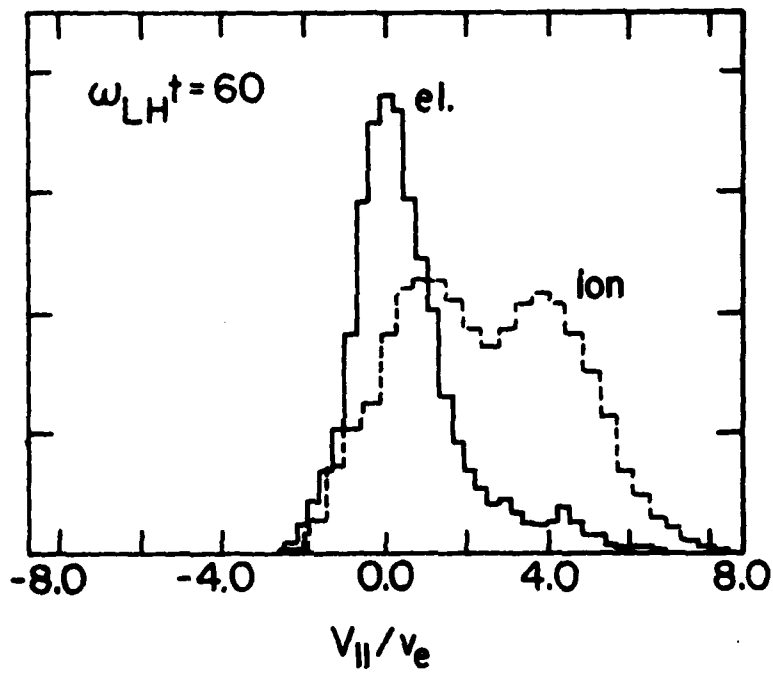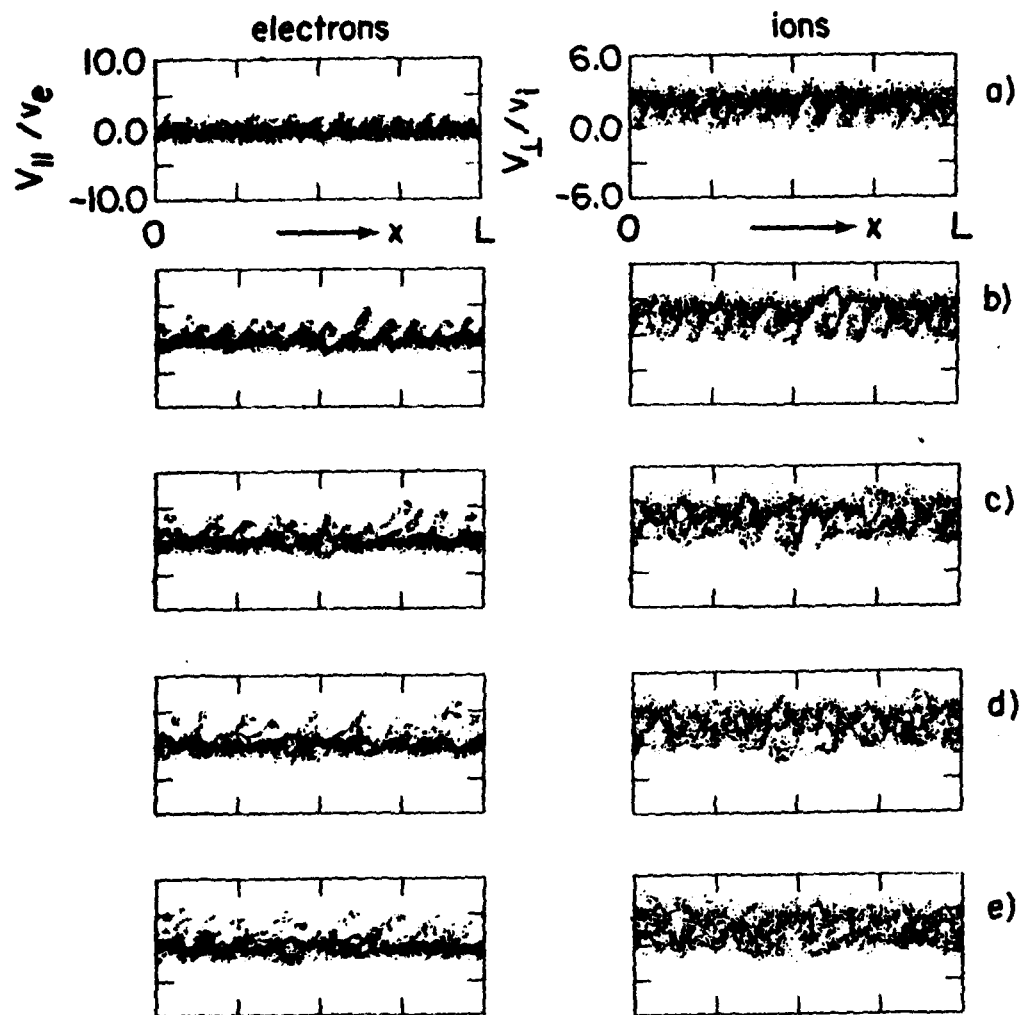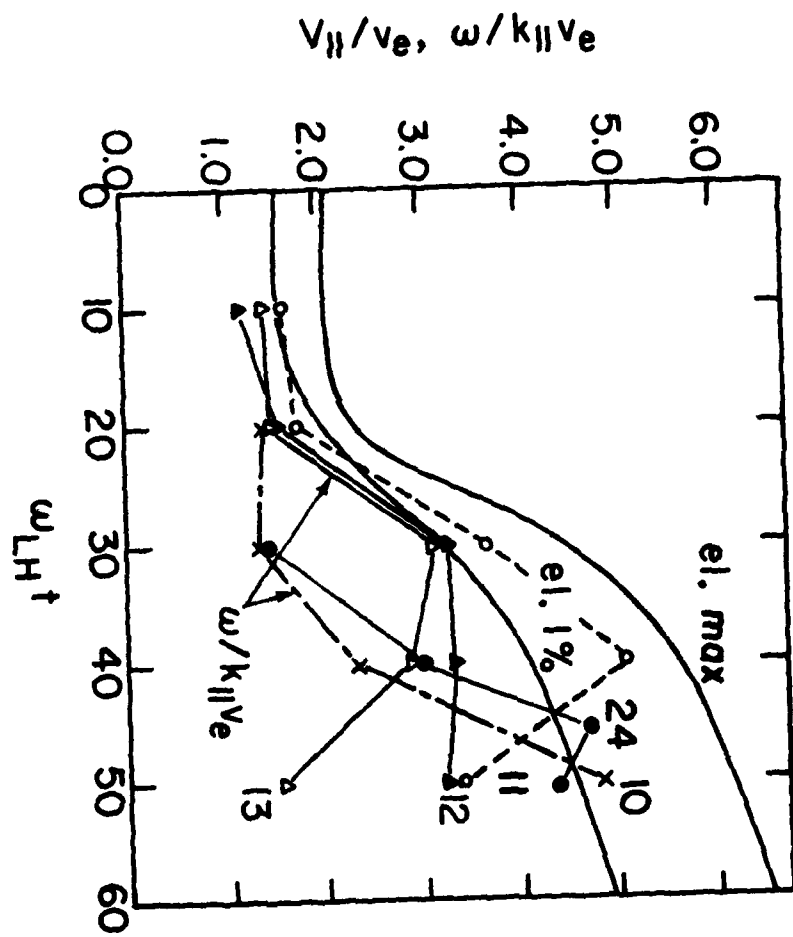
Fig. 3

Fig. 4